Performance investigation of uniaxially strained phosphorene n-MOSFETs

Sungwoo Jung, Junbeom Seo, Seonghyun Heo, and Mincheol Shin
School of Electrical Engineering
Korea Advanced Institute of Science and Technology
Deajeon, Republic of Korea
tjddn9988@kaist.ac.kr, jbseo@kaist.ac.kr, seonghyunheo@kaist.ac.kr, mshin@kaist.ac.kr

***Abstract*—In this work, we report on the performance of uniaxially strained monolayer black phosphorus (phosphorene) n-MOSFETs by first-principles-based quantum transport simulations. First, without applying strain, armchair direction (AD) FETs show better performance than zigzag direction (ZD) FETs due to the orientation-dependent transport characteristics that are attributed to the anisotropic band structure of phosphorene. With increasing tensile strain in AD, however, there occurs a downward shift of the conduction band (CB) at Y where the electron effective mass is light (heavy) in ZD (AD), resulting in an increase (decrease) in ON-state current (I_{ON}) of ZD (AD) FET. For the case of tensile strain in ZD, a sharp increase (decrease) in I_{ON} of ZD (AD) FET was observed. This is mainly due to band switching between the first and second conduction bands and a CB at a point between Γ and X; CB here has an electron effective mass light enough to enhance the performance of ZD FET. Overall, compared to the compressive strain, the band structure of phosphorene is more sensitive to the tensile strain in both directions, making it possible to improve the performance of ZD FET up to the level of AD FET.**

Keywords—Black phosphorus, anisotropic band strucutre, strain, n-MOSFETs.

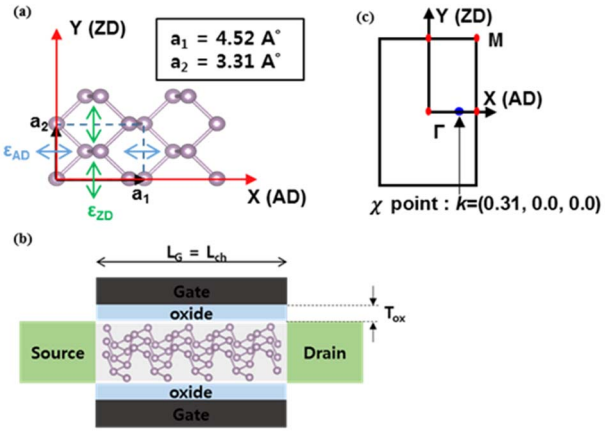

Fig. 1. (a) Top view of phosphorene. The dashed rectangle indicates the primitive cell lattice constants, a_1= 4.52 Å, a_2= 3.31 Å; we set the strain directions of X and Y for armchair and zigzag directions, respectively. (b) Schematic diagram of the phosphorene n-MOSFETs. (c) 2D Brillouin Zone for phosphorene.

I. Introduction

In recent decades, mainly because of their distinctive electronic and optical properties, 2D materials have drawn extensive interest and have become promising candidates for future electronics applications [1], [2]. Among 2D materials, black phosphorus (BP) has been widely explored because it displays electronic properties superior to those of its competitors, namely graphene and transition metal dichalcogenides (TMDs). For example, monolayer BP (phosphorene) inherently possesses a highly anisotropic band structure that arises from its puckered honeycomb structure [3]. Moreover, it exhibits higher mobility than that of TMDs and has a direct band gap that can be easily tuned by the thickness of the structure, which enhance its capability for nanoelectronic applications [4].

It is quite clear that the tunability of the electronic properties of semiconductors is a crucial aspect in terms of applications for nanoscale semiconductor devices. With the ultimate goal of enhancing device performance, strain engineering has generally been used to tailor electronic properties by means of various approaches, such as lattice mismatch, functional wrapping [5], [6], material doping [7], [8] and direct mechanical application [9] . Recent studies on strain engineering have suggested that phosphorene shows dramatic variations in electronic properties, such as band gap and carrier effective mass, under various strain conditions [10]. Following the studies dealing with the effects of strain on electronic properties, continuous attempts have been made to analyze the effect of varying strain on the performance of phosphorene devices by carrying out quantum transport simulations. For example, a computational investigation was conducted on the device performance of strained BP based MOSFETs. Transport properties were assessed under a moderate region of strain (-3% to +3%) with the effective mass Hamiltonian [11].

However, the effects of strain on the transport characteristics under higher levels of strain, which the device performance is expected to change more severely, have not been thoroughly studied yet. In this work, we conducted a theoretical study of

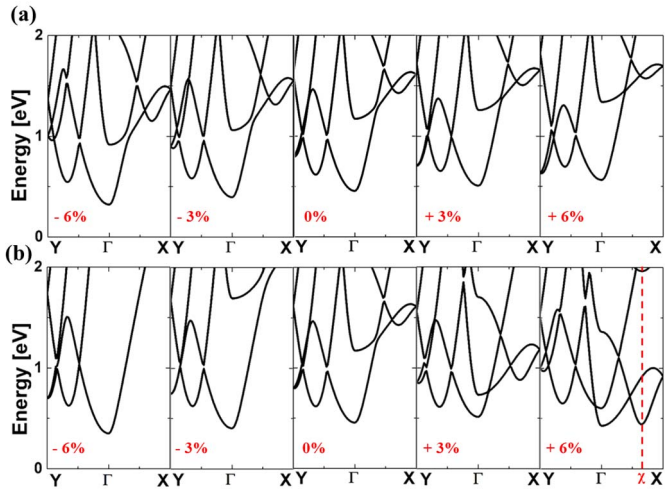

Fig. 2. Band structures of phosphorene under uniaxial strain (a) ε_{AD} and (b) ε_{ZD}. Band structures for the strains of 0%, ±3%, and ±6% are selectively plotted to clarify the changes under strain.

uniaxially strained phosphorene n-type MOSFETs using first-principles-based quantum transport simulations, taking into account the full band structure of phosphorene under various strain conditions.

II. Simulation Details

For the geometry optimization, first-principles density functional theory (DFT) calculations were carried out on the basis of a linear combination of atomic orbitals (LCAO) and using the OpenMX code [12]. We chose a $3s^1 3p^3 2d^5 1f^7$ LCAO basis set and generalized gradient approximation (GGA) exchange-correlation functional by Perdew, Burke, and Ernzerhof was adopted [13]. We employed a 10×10×1 *k*-grids and the atomic structures of strained phosphorene were fully relaxed until the maximum force reached 10^{-4} Hartree/Bohr. Fig. 1(a) presents the calculated lattice constants for phosphorene which are $a_1 = 4.52$ Å and $a_2 = 3.31$ Å, and in good agreement with the values of other theoretical works [4], [14]. With a fully relaxed structure of phosphorene, strain was gradually applied in either the AD or ZD, within the range of ±6%; these strains are denoted as ε_{AD} and ε_{ZD}, respectively. Especially when strain was applied in ZD, a negative Poisson ratio was observed, which originated from the puckered structure; this result is in-line with those of other theoretical studies [15], [16].

After validating our calculation results, non-orthogonal DFT Hamiltonians were extracted for each strained structure. Note that, to achieve the computational efficiency, the sizes of the Hamiltonians were reduced by a mode-space transformation, as presented in [17]. Next, to analyze the transport characteristics of phosphorene n-MOSFETs, we performed quantum transport calculations; a schematic diagram of our results is provided in Fig. 1(b). The channel length (L_{ch}) and equivalent oxide thickness (oxide thickness (T_{ox}) is set to 1.0 nm with relative dielectric constant of 1.12 for phosphorene [18]) are 10 nm and

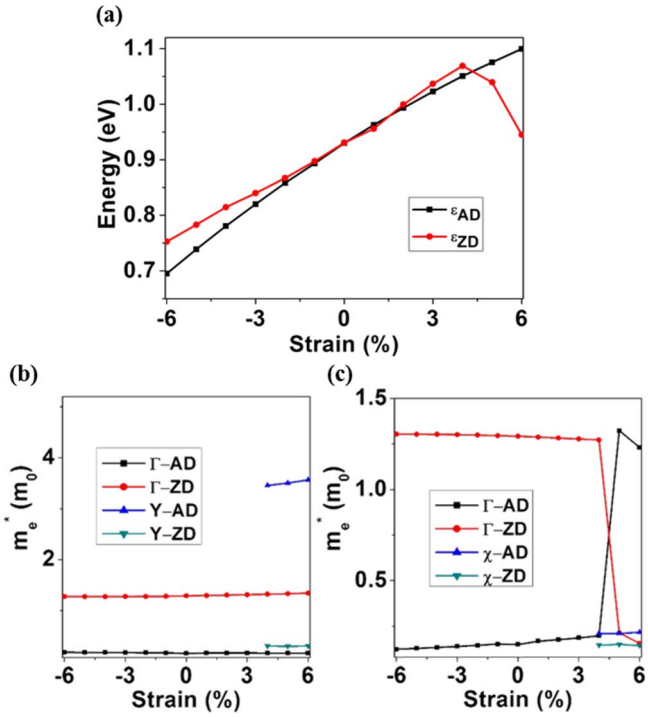

Fig. 3. (a) Band gap is plotted as a function of both ε_{AD} and ε_{ZD}. m_e^* under strain (b) ε_{AD} and (c) ε_{ZD}. Γ-AD (or ZD) denotes m_e^* of the CB at Γ for each direction and similar notation holds for CB at Γ and χ (Y-AD and χ-AD).

0.5 nm, respectively. Source and drain are n-doped with a density of 1×10^{21} cm^{-3}. DFT Hamiltonians of reduced size were imported into our in-house tool to compute the current and charge densities by self-consistently solving the non-equilibrium Green's function and the Poisson equation [17].

III. Band Structure of Strained Phosphorene

Fig. 2(a) and (b) illustrate the anisotropic band structures of phosphorene under two different strains, ε_{AD} and ε_{ZD}, respectively. The band structure was described along the band path of Y-Γ-X, as shown in Fig. 1(c). For unstrained phosphorene, there is a direct band gap, evaluated at 0.92 eV, which is in agreement with other *ab-initio* studies [4], [19]. As is already widely known, DFT-GGA functional underestimates the band gap of semiconductors: experimentally reported value of band gap is 1.45 eV [20]. Even with this underestimation, however, it is expected that our DFT results are meaningful because we are focused on the general trends of the effects of strain on the band structure and transport properties.

The band gap of phosphorene is plotted in Fig. 3(a) as a function of both ε_{AD} and ε_{ZD}. First, the band gap shows a gradual decrease with the increase of compressive ε_{AD}; this decrease of band gap is attributed to a downward shift of CB at Γ. A similar tendency of decreasing band gap can also be seen under compressive ε_{ZD}. With increasing tensile strain, the band gap

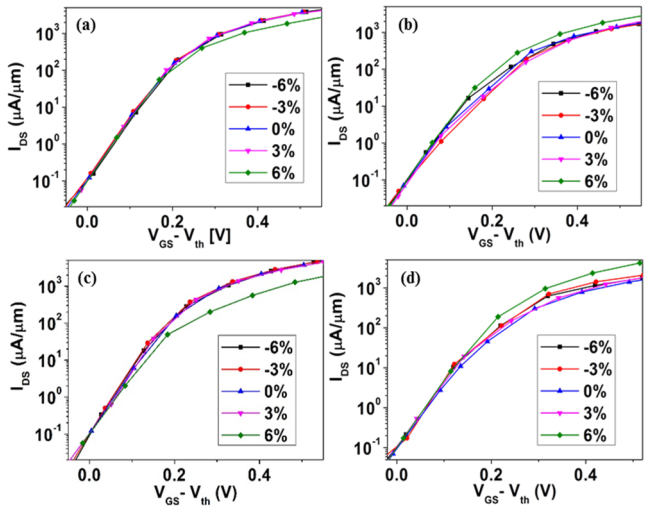

Fig. 4. Transfer characteristics of phosphorene n-MOSFETs under various strain conditions: (a) ε_{AD}-AD FET, (b) ε_{AD}-ZD FET, (c) ε_{ZD}-AD FET, and (d) ε_{ZD}-ZD FET. Note that the subscript of ε_{AD} (or ε_{ZD}) refers to the direction of applied strain, whereas AD (ZD) FET refers to the phosphorene n-MOSFETs whose transport direction is AD (ZD).

monotonically increases under ε_{AD} as CB moves away from the Fermi level, whereas with tensile ε_{ZD}, the band gap starts to decline after its peak around ε_{ZD} = +4% due to band switching between the first and second conduction bands.

The effective masses of electrons (m_e^*) are obtained from the curvature of the band structure. Fig. 3(b) and (c) show the alterations of m_e^* under ε_{AD} and ε_{ZD}, respectively. Regarding compressive strain, no significant change in m_e^* is observed under either ε_{AD} or ε_{ZD}, indicating the orientation dependence of phosphorene where m_e^* along ZD is larger than that along AD [21]. Under tensile ε_{AD}, however, there occurs a downward shift of CB at Y, for which m_e^* is light (heavy) in ZD (AD). For instance, at ε_{AD} = +6%, the energy gap between the conduction band minimum (CBM) at Γ and the conduction band edge (CBE) at Y narrows to 0.062 eV. For tensile ε_{ZD}, band switching takes place around ε_{ZD} = +4%, bringing sudden changes of m_e^* in both AD and ZD. With further increased tensile ε_{ZD}, CB at k = (0.31, 0.0, 0.0), denoted as χ, with small m_e^* in both AD and ZD, changes notably. For instance, the value of CBE at χ becomes comparable to that of CBM at ε_{ZD} = +6%, as plotted in Fig. 3(c).

IV. PHOSPHORENE n-MOSFETS SIMULATION RESULTS

Fig. 4 shows the transfer curves of uniaxially strained phosphorene n-MOSFETs. Curves are shifted to have an OFF-state current (I_{OFF}) of 10^{-1} μA/μm at V_{GS} = 0 V, which is a ITRS requirement for high performance in the I_{OFF} specifications [22]. Transfer curves for strains of 0%, ±3%, and ±6% are selectively plotted. Although I_{ON} rarely changes in the first two cases, an appreciable decrease and an appreciable increase are observed from AD FET and ZD FET, respectively under strong tensile ε_{ZD}, as can be seen in Fig. 4(c) and (d).

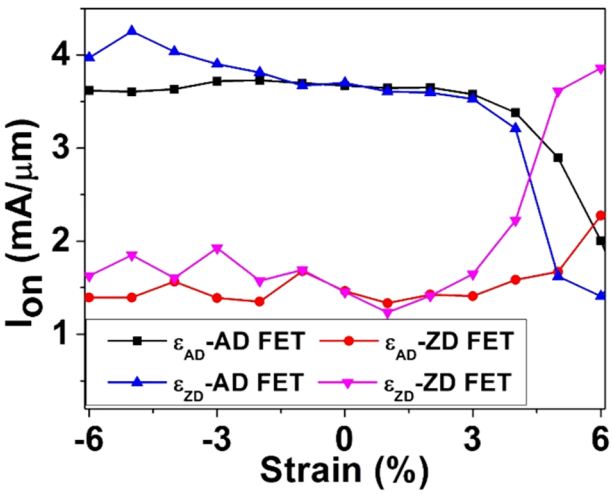

Fig. 5. I_{ON} of the n-MOSFET as a function of uniaxial strain. I_{ON} is defined at V_{GS}-V_{th} = V_{DS} = 0.5 V, where the OFF-state current is set at 10^{-1} μA/μm

To clarify the variations in transport characteristics, the values of I_{ON} of n-MOSFETs with two different transport directions, AD FET and ZD FET, as a function of strains ε_{AD} and ε_{ZD}, are shown in Fig. 5. Here, I_{ON} is defined at $V_{GS} - V_{th} = V_{DS}$ = 0.5 V. As can be expected from the results in section Ⅲ, no noticeable change of I_{ON} occurs for either compressive ε_{AD} or ε_{ZD}, since there was little change in m_e^* (see Fig. 3(b) and (c)).

However, it is found that AD FET under strong tensile ε_{AD} (ε_{AD}-AD FET) shows a rapid decline in I_{ON} because a CB at Y, whose m_e^* is heavy in AD, begins to contribute to I_{ON} at ε_{ZD} = +4%. On the contrary, ZD FET under the same strain condition (ε_{AD}-ZD FET) shows a moderate improvement in I_{ON} owing to the small value of m_e^* at Y in ZD. For the case of tensile ε_{ZD}, there occurs a sharp increase (decrease) in I_{ON} of ε_{ZD}-ZD (AD) FET around ε_{ZD} = +4%, which can be explained by the decrease (increase) of m_e^* along ZD (AD), resulting from band switching. Particularly, ε_{ZD}-ZD FET under strong tensile ε_{ZD} exhibits the greatest improvement in I_{ON}; this improvement is attributed to not only band switching but also to the CB at χ, with light m_e^*, which contributes dominantly to improving I_{ON}.

V. CONCLUSION

A detailed study of strain effect on uniaxially strained phosphorene n-MOSFETs was performed by means of DFT-based self-consistent quantum transport simulations. We identified the variations of band structures with various strains, and found that these strain effects directly lead to alterations in the performance of phosphorene FETs. Overall, it is likely that tensile strain applied in either direction is more useful than compressive strain in modifying the electronic properties of phosphorene. Consequently, we emphasize that the strain engineering can be an effective way to modulate the effective mass of phosphorene, making it possible to narrow the performance gap between AD and ZD FETs.

ACKNOWLEDGMENT

This research was supported by the Development of Million-Atom First-principles Simulator for Nano Transistor Devices through the National Research Foundation of Korea (NRF) funded by the Ministry of Education, Science and Technology (Grant No.NRF-2017R1A2B2005679).

REFERENCES

[1] K. S. Novoselov, A. K. Geim, S. V. Morozov, D. Jiang, M. I. Katsnelson, I. V. Grigorieva, S. V. Dubonos, and A. A. Firsov, "Two-dimensional gas of massless Dirac fermions in graphene," *Nature*., vol. 438, pp. 197-200, Nov. 2005, doi: 10.1038/nature04233.

[2] B. Radisavljevic, A. Radenovic, J. Brivio, V. Giacometti, and A. Kis, "Single-layer MoS2 transistors," *Nature Nanotechnol*., vol. 6, pp. 147-150, Mar. 2011, doi: 10.1038/NNANO.2010.279.

[3] XB. Li, P. Guo, TF. Cao, H. Liu, WM. Lau, and LM. Liu, "Structures, stabilities, and electronic properties of defects in monolayer black phosphorus," *Sci. Rep*., vol. 5, pp. 10848-1-10848-11, May. 2015, doi: 10.1038/srep10848.

[4] H. Liu, A. T. Neal, Z. Zhu, Z. Luo, X. Xu, D. Tománek, and P. D. Ye, "Phosphorene: an unexplored 2D semiconductor with a high hole mobility," *ACS Nano*, vol. 8, no. 4, pp. 517-521, Mar. 2014, doi: 10.1021/nn501226z.

[5] A. Thean, and J. P. Leburton, "Strain effect in large silicon nanocrystal quantum dots," *App. Phys. Lett*., vol.79, pp. 1030-1032, Aug. 2001, doi: 10.1063/1.1392309.

[6] X. L. Wu, and F. S. Xue, "Optical transition in discrete levels of Si quantum dots," *App. Phys. Lett*., vol 84, pp. 2808-2810, Apr. 2004, doi: 10.1063/1.1704872.

[7] L. Seravalli, M. Minelli, P. Frigeri, P. Allegri, V. Avanzini, and S. Franchi, "The effect of strain on tuning of light emission energy of InAs/InGaAs quantum-dot nanostructures," *App. Phys. Lett*., vol. 82, pp. 2341-2343, Apr. 2003, doi: 10.1063/1.1566463.

[8] S. Mazzucato, D. Nardin, M. Capizzi, A. Polimeni, A. Frova, L. Seravalli, S. Franchi, "Defect passivation in strain engineered InAs/(InGa) As quantum dots," *Mater. Sci. Eng., C*, vol. 25, pp. 830-834, Dec. 2005, doi: 10.1016/j.msec.2005.06.025.

[9] Y. G. Wang, Q. L. Zhang, T. H. Wang, W. Han, and S. X. Zhou, "Improvement of electron transport in a ZnSe nanowire by in situ strain," *J. Phys. D: Appl. Phys*., vol. 44, pp. 125301-1-125301-7, Mar. 2011, doi: 10.1088/0022-3727/44/12/125301.

[10] X. Peng, Q. Wei, and A. Copple, "Strain-engineered direct-indirect band gap transition and its mechanism in two-dimensional phosphorene," *Phys. Rev. B*, vol. 90, pp. 085402-1-085402-10, Aug. 2014, doi: 10.1103/PhysRevB.90.085402.

[11] L. Banerjee, A. Mukhopadhyay, A. Sengupta, H. Rahaman, "Performance analysis of uniaxially strained monolayer black phosphorus and blue phosphorus n-MOSFET and p-MOSFET," *J. Comput. Eletron*., vol. 15, pp. 919-930, Jun. 2016, doi: 10.1007/s10825-016-0846-x.

[12] T. Ozaki, and H. Kino, "Efficient projector expansion for the ab initio LCAO method," *Phys. Rev. B*., vol. 72, pp. 045121-1-045121-8, Jul. 2005, doi: 10.1103/PhysRevB.72.045121.

[13] J. P. Perdew, K. Burke, and M. Ernzerhof, "Generalized gradient approximation made simple," *Phys. Rev. Lett*. Vol. 72, pp. 3865-3868, May. 2016, doi: 10.1103/PhysRevLett.77.3865.

[14] J. Qiao, X. Kong, ZX. Hu, F. Y, and W. Ji, "High-mobility transport anisotropy and linear dichroism in few-layer black phosphorus," *Nature Commun*., vol. 5, pp. 4475-1-4475-7, Jul. 2014, doi: 10.1038/ncomms5475.

[15] J. W. Jiang, and H. S. Park, "Negative poisson's ratio in single-layer black phosphorus," *Nature Commun*., vol. 5, pp. 1-7, Jul. 2014, doi: 10.1038/ncomms5727.

[16] J. Du, J. Maassen, W. Wu, Z. Luo, X. Xu, and P. D. Ye, "Auxetic black phosphorus: a 2D material with negative poisson's ratio," *Nano Lett*, vol. 16, pp. 6701-6708, Sep. 2016, doi: 10.1021/acs.nanolett.6b03607.

[17] M. Shin, W. J. Jeong, and J. Lee, "Density functinoal theory based simualtions of silicon nanowire field effect transistors," *J. Appl. Phys*., vol. 119, pp. 154505-1-154505-10, Apl. 2016. doi: 10.1063/1.4946754.

[18] V. Wang, Y. Kawazoe, and W. T. Geng, "Native point defects in few-layer phosphorene," *Phys. Rev. B*, vol. 91, pp. 045433-1-045433-9, Jan. 2015, doi: 10.1103/PhysRevB.91.045433.

[19] V. Tran, R. Soklaski, Y. Liang, and L. Yang, "Layer-controlled band gap and anisotropic excitons in few-layer black phosphorus," *Phys. Rev. B*, vol. 89, pp. 235319-1-235319-6, Jun. 2014, doi: 10.1103/PhysRevB.89.235319.

[20] X. Wang, A. M. Jones, K. L. Seyler, V. Tran, Y. Jia, H. Zhao, H. Wang, L. Yang, X. Xu, and F. Xia, "Highly anisotropic and robust excitons in monolayer black phosphorus," *Nature nanotechnol*., vol. 10, pp. 517-521, Jun. 2015, doi: 10.1038/nnano.2015.71.

[21] J. Chang, and C. Hobbs, "Theoretical study of phosphorene tunneling field effect transistors," *Appl. Phys. Lett*., vol. 106, pp. 083509-1-083509-5, Feb. 2015, doi: 10.1063/1.4913842.

[22] Internationals Technology Roadmaps for Semiconductor (ITRS-2013) Report. [Online]. Available: http://www.itrs2.net/